RESEARCH ARTICLE

Distributed Practical Prescribed-Time Secondary Control of Microgrid under Event-Triggered Communication

Houlang He[1,2,3], **Yu Zhou**[1,2,3], **Guanghui Jiang**[1,2,3] **and Leimin Wang**[1,2,3,*]

[1] School of Automation, China University of Geosciences, Wuhan 430074, China
[2] Hubei Key Laboratory of Advanced Control and Intelligent Automation for Complex Systems, Wuhan 430074, China
[3] Engineering Research Center of Intelligent Technology for Geo-Exploration, Ministry of Education, Wuhan 430074, China

Abstract

With the increasing integration of distributed generation into the grid, the secondary control of microgrids has become a prominent research focus in this field. However, distributed secondary control in microgrids is subject to constraints from external factors, necessitating both rapid response speed and a reliable communication network. This paper proposes a distributed practical prescribed-time secondary control method aimed at achieving microgrid stability. A key feature of this approach is that the convergence time can be predefined and remains independent of both design parameters and initial conditions. Furthermore, an event-triggered communication strategy is adopted to enhance the efficiency of communication resource utilization within the microgrid. The criterion for achieving practical prescribed-time consensus in the microgrid is established using Lyapunov stability theory. Moreover, the proposed distributed secondary control method is proven to exclude Zeno behavior. Finally, the effectiveness and superiority of the proposed method are demonstrated through case analyses and simulation results.

Keywords: microgrid, distributed secondary control, event-triggered mechanism, practical prescribed-time consensus.

1 Introduction

Energy drives industrial development, with electricity being a widespread, efficient and clean source of energy. With the increasing depletion of fossil fuels as the main source of electricity, the development of renewable energy is critical for the future [1]. Renewable energy sources are frequently located in remote areas away from loads and required distributed generation (DG) technologies. DG includes renewable and other energy sources, easing the pressure on energy supply. Intermittent generation from DG causes challenges in system operation as it affects the stability of the grid [2].

In order to reply the challenges of DG, the concept of microgrid is introduced, aiming to enhance grid-connected operation and increase renewable energy absorption [3]. Despite its benefits, microgrid control faces challenges such as small inertia and slow dynamic response. Traditional centralized control manages all DGs from a central center. In contrast,

Submitted: 03 August 2025
Accepted: 08 September 2025
Published: 15 September 2025

Vol. 1, **No.** 1, 2025.
10.62762/JNDA.2025.939275

***Corresponding author:**
✉ Leimin Wang
wangleimin@cug.edu.cn

Citation
He, H., Zhou, Y., Jiang, G., & Wang, L. (2025). Distributed Practical Prescribed-Time Secondary Control of Microgrid under Event-Triggered Communication. *Journal of Nonlinear Dynamics and Applications*, 1(1), 36–51.

distributed control equips each DG with local control algorithms and establishes a communication network. Distributed control reduces costs, enhances reliability, and compensates for centralized control shortcomings.

Distributed secondary control of microgrid is a typical application scenario of multi-agent system (MAS) consensus algorithm [4]. The microgrid system with multiple DGs can be regarded as a MAS, and each DG is an autonomous agent. By selecting different transmission variables, the MAS consensus algorithm can be used to achieve different control objectives in the microgrid [5]. The design of an effective distributed secondary control strategy is of great theoretical significance and application value in order to improve the distributed control performance of a microgrid.

The consensus time of the controlled state serves as a crucial indicator of the quality of the control algorithm in microgrid [6]. Currently, the majority of distributed secondary control strategies can only attain asymptotic consensus of the controlled state, leading to extended convergence times and increased steady-state errors in practical applications. Therefore, the concept of finite-time consensus in the field of microgrid has been introduced, which refers to the controlled state converging to the target value within a finite time range [7]. Consequently, the corresponding distributed secondary control strategy has been designed for this purpose.

In [8], a distributed MAS finite-time method was proposed allowing for time delay. In [9], a distributed finite-time secondary control method was proposed considering unknown perturbations and uncertainties in the model. In [10], the finite-time voltage secondary control and power generation cost control for microgrid were designed, addressing voltage regulation and cost optimization challenges.

The finite-time consensus has been shown to reduce the convergence time of the controlled state and improve the accuracy of steady-state control. However, the settling time of finite-time consensus is contingent on the initial value of the controlled state. Due to the random nature of the initial value, adjusting the settling time is challenging. For this reason, the fixed time was proposed which has the advantage that the settling time of fixed-time consensus is not depend on the initial values [11]. Moreover, the fixed-time consensus has received extensive attention in the secondary control of the microgrid [12–14].

A distributed fixed-time secondary controller was devised to improve dynamic performance of the microgrid within a fixed time in [15]. In [16], a distributed fixed-time secondary controller was proposed with the aim of eliminating DC voltage deviation. The objective of this was to improve the operational performance of microgrids in both steady state and transient states. A distributed fixed-time secondary control scheme based on dynamic averaging consensus was investigated in [17], which realizes the current sharing between converters and the voltage regulation of the DC bus in a fixed time.

Even though the settling time of the fixed-time is independent of the initial value of the controlled state, it has a complex relationship with system and controller parameters that cannot be easily predefined [18]. Overall, from the above analysis, it can be seen that although the control strategies based on finite/fixed-time consensus largely shorten the consensus time and improve the general control performance of the microgrid system, the range of the consensus time often relies on the parameters of the system, which is not easy to be adjusted according to the actual demand. On the other hand, in the hierarchical control of microgrids, the time scale between layers is very important. If the consensus time of the controlled state can be determined in advance without preconditions, the control performance of the whole microgrid will be further improved. Therefore, the study of prescribed-time consensus for microgrid can predefine the consensus time for the secondary control of microgrid without prerequisites, further realizing more stable operation of microgrid.

In addition, the distributed secondary control of microgrids not only relies on the convergence time of the consensus algorithm, but also depends on the real-time performance of communication networks. However, communication networks are in reality susceptible to various forms of communication constraints that degrade their transmission performance and in severe cases even lead to the operational collapse of ancillary systems [19–21]. Furthermore, information interaction between controlled objects requires not only accessing information from neighbouring nodes, but also executing control decisions locally. Therefore, multiple aspects in distributed control are affected by the impact caused by communication constraints.

The event-triggered mechanism is regarded as an essential mean to cope with the communication

resource constraints due to their non-periodic intermittent information transmission method that can save communication and computation resources to a great extent. In this regard, the study of distributed control of microgrid based on event-triggered communication mechanism has attracted extensive attention [22–24]. In order to reduce the number of controller updates in [22], an event-triggered frequency modulation and voltage regulation based method was proposed. In [23], a power secondary controller based on event-triggered communication was designed with the objective of economic distribution of active power. In [24], an event-triggered communication mechanism is applied to frequency and voltage restoration in an islanded microgrid.

Event-triggering mechanisms can be combined with existing consensus control algorithms to reduce the communication resource requirements of distributed control systems [25–27]. However, for relatively complex distributed control strategies, it is difficult to design the threshold function of event triggered conditions, and improper design leads to Zeno behaviour or even destroy the convergence of the system. Yu in [28] revealed the essential contradiction between event-triggered mechanism and finite-time control. It is obvious that when the time converges to the settling time, the controller will be updated at a faster frequency, which may lead to Zeno behavior if the event-triggered mechanism is not properly designed. Therefore, it is worthwhile to design a reasonable event triggered mechanism to avoid the Zeno behavior needs to be further discussed.

The practical applications of microgrids regularly require optimising consensus time and saving communication resources. Therefore, this paper proposes a practical prescribed-time consensus algorithm based on the event-triggered mechanism for distributed secondary control of microgrids. The main contributions are as follows

1) A distributed practical prescribed-time secondary control method is proposed to achieve microgrid stabilisation at a prescribed time. Compared with previous fixed-time consensus controllers [15–17], the structure of the controller is greatly simplified. On the other hand, the method proposed in this paper not only reduces the conservatism of the estimated time, but also avoids the controller from generating excessive inputs. The designed controllers are more in line with the reality of microgrids.

2) A new event-triggered communication mechanism is designed to solve the problem of tight communication resources in microgrids. The time base generator function is introduced in the design of event-triggered conditions. Compared with the event-triggered mechanism with absolute threshold [27], the event-triggered mechanism in this papre can further reduce the triggering rate. In addition, due to our faster convergence, our event-triggered moments are sparser than the traditional ones when the time is larger than the prescribed time, which can further reduce the consumption of communication resources.

3) The secondary control of microgrids is greatly dependent on the communication network. In [25–27], the Zeno behaviour was not excluded at $t = t_p$, which is harmful to communication network, this conclusion is not applied to microgrids. In this paper, our method ensures that the Zeno behavior can be drained at any moment, further enhancing the quality of the microgrid communication network.

The remainder of this paper is organized as follows. Section II presents the preliminary framework and formulates the microgrid control problem. In Section III, we develop distributed secondary control algorithms for frequency and voltage regulation, along with theoretical analysis demonstrating their stability and convergence properties. Section IV provides comprehensive simulation results to validate the efficacy of the proposed control scheme. Finally, Section V concludes the paper with key findings and potential directions for future research.

2 Model and Preliminaries

2.1 Graph Theory

Consider an undirected graph $\mathcal{G}$ consisting of N agents, where each agent corresponds to a node. The set of edges $\mathcal{V}$ defines the communication links between agents. If $(j,i) \in \mathcal{V}$, agents i and j are neighbors and can exchange information bidirectionally. The adjacency matrix $\mathcal{A} = [a_{ij}] \in \mathbb{R}^{N\times N}$ is defined such that $a_{ij} = \begin{cases} 1, \text{if } (j,i) \in \mathcal{V} \\ 0, \text{ otherwise} \end{cases}$. The degree matrix $\mathcal{D} = \text{diag}(d_1, \ldots, d_N)$ is a diagonal matrix where $d_i = \sum_{j\neq i} a_{ij}$. The Laplacian matrix $\mathcal{L} = [l_{ij}] \in \mathbb{R}^{N\times N}$ of graph $\mathcal{G}$ is given by $\mathcal{L} = \mathcal{D} - \mathcal{A}$. Moreover, the graph $\mathcal{G}$ is said to be connected if there exists a path between any two distinct nodes.

2.2 Modeling and Control of the Inverter-Based Microgrid

The primary control of microgrids usually employs a droop control strategy that simulates the external characteristics of generators. The droop equation is expressed as [21]

$$\begin{cases} \omega_i = \omega_i^n - k_i^P P_i, \\ v_i^{od} = v_i^n - k_i^Q Q_i, v_i^{oq} = 0 \end{cases} \tag{1}$$

where ω_i denote the angular frequency magnitude, while v_i^{od} and v_i^{oq} represent the d-axis and q-axis voltage components, respectively. The nominal setpoints for frequency and voltage are given by ω_i^n and v_i^n. The active and reactive power outputs are denoted by P_i and Q_i, with k_i^P and k_i^Q being the corresponding droop coefficients for primary control. Besides, the terminal voltage is $v_i = \sqrt{\left(v_i^{od}\right)^2 + \left(v_i^{oq}\right)^2}$. Let v_i replace v_i^{od} in the following paper.

Microgrids regulate the output of each DG by varying the frequency and voltage magnitude via droop control in order to quickly reach an internal supply-demand balance when the system is disturbed. Therefore, it is necessary to add a secondary control to the primary control to eliminate the offsets.

Distributed control combined with MAS is usually considered in the secondary control of microgrids [21]. As shown in Figure 1, four different DGs units, the main grid unit and the load unit are included in this control model. Each DG is considered as an independent agent. The agents receive measured data from the inverter to perform secondary control, in addition to establishes a communication network for all DGs. The agents receive measurement data from the inverter, performs secondary control as well as setting up the communication network for all DGs.

In order to realise the distributed secondary control of microgrids using the MAS consensus algorithm, it is necessary to first differentiate the droop equation in Equation (1) and then design a control law to find the derivatives of the controlled state

$$\begin{cases} \dot{\omega}_i = u_i^{\omega}, \\ \dot{v}_i = u_i^{v}, \\ \dot{\omega}_i = \dot{\omega}_i^n - k_i^P \dot{P}_i, \\ \dot{v}_i = \dot{v}_i^n - k_i^Q \dot{Q}_i, \end{cases} \tag{2}$$

in which u_i^{ω}, u_i^{v} are the frequency and voltage secondary control signals to be designed, $\dot{P}_i = \omega_i^c \left(v_i^{od} i_i^{od} - v_i^{oq} i_i^{oq}\right) - \omega_i^c P_i$ and $\dot{Q}_i = \omega_i^c \left(v_i^{od} i_i^{oq} - v_i^{oq} i_i^{od}\right) - \omega_i^c Q_i$ are taken from [16], and ω_i^c is the cut-off frequency of the low-pass filter. According to (2), ω_i^n and v_i^n can be obtained as follows

$$\begin{cases} \omega_i^n = \int_0^t u_i^{\omega}(r) + k_i^P u_i^p(r) dr, \\ v_i^n = \int_0^t u_i^v(r) + k_i^Q \dot{Q}_i(r) dr. \end{cases} \tag{3}$$

In practice, the secondary control is used to correct for frequency and voltage deviations by adjusting the reference calibration values ω_i^n and v_i^n in the droop control. This eliminates the bias generated by the primary control.

2.3 Time Base Generator Function

According to [29], the time base generator function (TBG) is given as follows

$$k(t) = \frac{\dot{\xi}(t)}{1 - \xi(t) + \sigma}, \tag{4}$$

where $\xi(t)$ is the TBG, and $0 < \sigma \ll 1$. It is required that $\xi(t)$ holds the following generalized properties:

1) $\xi(t)$ is at least C^2 on $(0, +\infty)$;

2) The function $\xi(t)$ is a continuous and monotonically non-decreasing function defined on $t \geq 0$, with initial condition $\xi(0) = 0$ that converges asymptotically to a terminal value $\xi(t_p) = 1$, where $t_p < +\infty$ is a prescribed time;

3) $\dot{\xi}(0) = \dot{\xi}(t_p) = 0$ (the derivative of $\xi(t)$ at $t = 0$ is in fact its right derivative);

4) When $t > t_p$, $\xi(t) = 1$ and thus $\dot{\xi}(t) = 0$.

2.4 Definition and Lemmas

Consider a multi-agent system consisting N agents with single-integrator dynamics. The state evolution of the i th agent, $i \in \mathcal{V} := \{1, 2, \ldots, N\}$, is governed by the following differential equation

$$\dot{x}_i(t) = u_i(t) \tag{5}$$

where $x_i(t) \in \mathbb{R}$ represents the state variable and $u_i(t) \in \mathbb{R}$ denotes the control input of agent i. The communication topology among agents is modeled as an undirected graph $\mathcal{G}$ represents the set of interaction edges.

Definition 1. For system (5), the practical prescribed-time consensus is achieved if for any

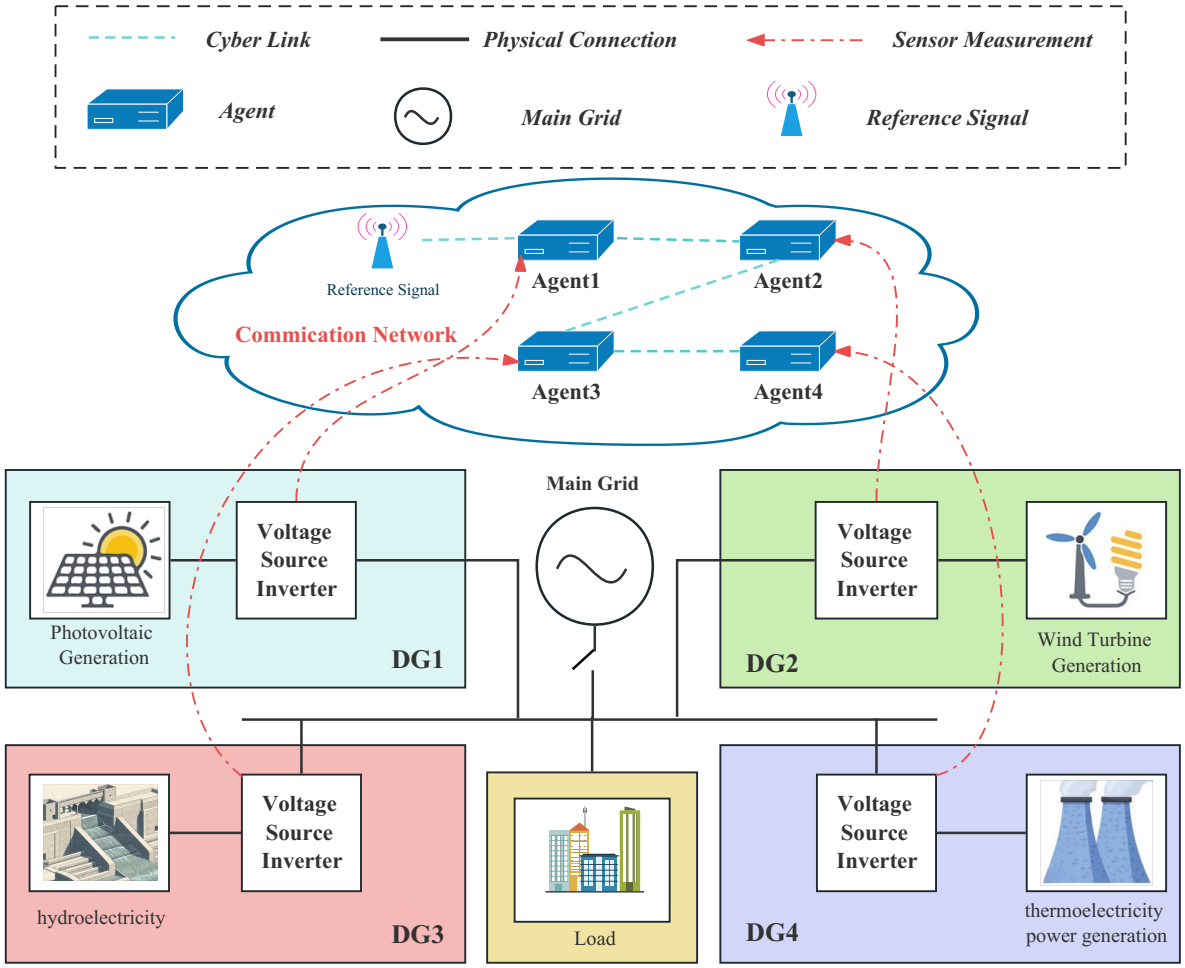

Figure 1. The cyber-physical structure of microgrid.

initial state $x_i(0), i \in \mathcal{V}$, there exists a settling time t_p and a bounded constant c such that

$$\begin{cases} \lim_{t\to t_p} |x_i(t) - x_j(t)| \le c, \\ |x_i(t) - x_j(t)| \le c, \ \forall t > t_p, \\ \lim_{t\to+\infty} |x_i(t) - x_j(t)| = 0, \end{cases} \tag{6}$$

where t_p and c are directly adjustable parameters in the control design.

Lemma 1 [30]. Assume the communication graph $\mathcal{G}$ among followers is undirected and connected. If there exists at least one directed edge from a follower to the leader, then the composite matrix $\hat{L} = L + B$ is symmetric and positive definite.

Lemma 2 [31]. Consider system (5), if there exist a continuously differentiable and positive-definite function $V : \mathbb{R}^N \to \mathbb{R}_+$, and a positive constant $\alpha > 0$, such that

$$\dot{V}(t) \le -(1 + k(t))\alpha V(t), \quad t \in [0, t_p) \tag{7}$$

and

$$\dot{V}(t) \le -\alpha V(t), \quad t \in [t_p, \infty). \tag{8}$$

Then, it holds that

$$V(t) \le e^{-\alpha t} \left(\frac{1 - \xi(t) + \sigma}{1 + \sigma} \right)^{-\alpha} V(0), \quad t \in [0, t_p] \tag{9}$$

and

$$\lim_{t\to+\infty} V(t) = 0. \tag{10}$$

Moreover, the origin of system (5) is practical prescribed-time stable with the settling time t_p.

Lemma 3 [32]. For any vectors $x, y \in \mathbb{R}^N$ and a positive constant $c \in \mathbb{R}$, the following inequality holds

$$x^T y \le \frac{1}{2} \left(c x^T x + \frac{1}{c} y^T y \right). \tag{11}$$

3 Main Results

3.1 Control Design

Distributed cooperative control of microgrid is a typical application scenario of MAS consensus algorithm. The microgrid system and the DG are considered as MAS and agent, respectively, then the frequency/voltage regulation problem in the

secondary control of microgrid can be regarded as the MAS leaders-follow consensus problem, which can be described as follows

$$\begin{cases} \lim_{t\to t_p} |\omega_i(t) - \omega^*| = \delta_1, \\ \lim_{t\to+\infty} |\omega_i(t) - \omega^*| = 0, \end{cases} \tag{12}$$

$$\begin{cases} \lim_{t\to t_p} |v_i(t) - v^*| = \delta_2, \\ \lim_{t\to+\infty} |v_i(t) - v^*| = 0, \end{cases} \tag{13}$$

where δ_1, δ_2 are positive constants that can be set in advance, and ω^*, v^* are target signals.

Considering Equation (4), the distributed prescribed-time secondary controller is designed as follows

$$\begin{aligned} u_i^{\omega}(t) &= (1+k(t))\,[\sum_{j\in N_i} a_{ij}\,(\omega_i(t) - \omega_j(t)) \\ &\quad + b_i\,(\omega_i(t) - \omega^*)], \\ u_i^{v}(t) &= (1+k(t))\,[\sum_{j\in N_i} a_{ij}\,(v_i(t) - v_j(t)) \\ &\quad + b_i\,(v_i(t) - v^*)]. \end{aligned} \tag{14}$$

Remark 1. In [33], the controller gain tends to infinity, this conclusion is not applicable to microgrid systems. In order to ensure that the controller output is bounded, it is necessary to satisfy that the product of the controller input signal and the controller gain is a bounded value, meaning that at this point the detected signal must converge to 0. However, in a power system, when electronic components are switched on and off, additional high frequency signals are generated, where the controller designed in [33] no longer satisfies the condition that the output is bounded. Compared to the infinite gain controller, the controller we consider avoids the singularity problem and is more in line with the practical requirements of power systems.

Remark 2. Different from the existing distributed finite/fixed-time control [9][12], we construct a distributed prescribed-time controller based on TBG function. At the beginning, the gain of the controller is small due to the TBG function. This strategy avoids the problem that the gain of the fixed-time controller is too large at the beginning. Moreover, as opposed to fractional order, exponential, and integral controllers, the distributed control strategy based on TBG function presented in this paper is continuous and smooth. In addition, since the simple design and calculation of time base generator $k(t)$, the distributed prescribed-time control strategy designed is simple in structure with easy implementation.

3.2 Event-Triggered Communication Mechanism

The frequency and voltage measurement errors of the i-th DG are defined as

$$\begin{cases} e_i^{\omega}(t) = \omega_i(t_k^i) - \omega_i(t), \\ e_i^{v}(t) = v_i(t_k^i) - v_i(t). \end{cases} \tag{15}$$

We define $e_i(t) = [e_i^{\omega}(t), e_i^{v}(t)]^T$. If the above measurement error of each DG reaches or exceeds the specified threshold, then the event is triggered and the node information can be re-measured and transmitted to update the control signal.

Accordingly, the event-triggered mechanism is defined as follows

$$t_{k_i+1}^i = \inf\left\{t : t \geq t_{k_i}^i, \kappa_i \vartheta_i(t) \geq \eta_i(t)\right\}, \tag{16}$$

where $\vartheta_i(t) = ||e_i(t)||^2$, $\kappa_i > 0$ and $\eta_i(t)$ is the threshold function defined by

$$\begin{aligned} &\eta_i(t) \\ &= e^{-\phi_i t}(1+\sigma-\xi(t))^{\phi_i} \\ &\left(\tau_i - \int_0^t (k(s)+1)\vartheta_i(s)e^{\phi_i s}(1+\sigma-\xi(s))^{-\phi_i} ds\right), \end{aligned} \tag{17}$$

where τ_i, ϕ_i are positive constants.

For each DG, the condition that its threshold function $\eta_i(t) > 0$ must be satisfied. We give the proof as follows.

Proof: By the definition of $\eta_i(t)$, its derivative is

$$\dot{\eta}_i(t) = (k(t)+1)\left(-\phi_i\eta_i(t) - \vartheta_i(t)\right). \tag{18}$$

In addition, from the defined trigger condition

$$\kappa_i\vartheta_i(t) < \eta_i(t). \tag{19}$$

Thus we can obtain

$$\dot{\eta}_i(t) > -\left(\phi_i + \frac{1}{\kappa_i}\right)(k(t)+1)\eta_i(t). \tag{20}$$

Unite with $\eta_i(0) = \tau_i(1+\sigma)^{\phi} > 0$, for every $t \geq 0$, we have

$$\eta_i(t) > \eta_i(0)e^{-(\phi_i+1/\kappa_i)}\left(1 - \frac{\xi(t)}{1+\sigma}\right)^{\phi_i+1/\kappa_i} > 0. \tag{21}$$

Therefore the trigger threshold we designed is reasonable. Proof completes.

Remark 3. Different from the absolute threshold event-triggered conditions [27], the threshold function

proposed in this paper contains the dynamic variable $\eta_i(t)$. This dynamically changing threshold can be used to further reduce the number of triggers. In addition, by introducing a time base generator function, the consensus time is predetermined and adjustable. This is in contrast to existing dynamic event-triggered mechanisms, which can only guarantee asymptotic convergence.

Remark 4. According to the definition of $k(t)$, there is $k(t) = 0$ when $t > t_p$. At this point, it is the same as the trigger condition in [34]. In contrast, with the introduction of $k(t)$, system can converge to the boundary in a much shorter time. This also implies that the error $\vartheta_i(t)$ in Equation (16) will be smaller when $t > t_p$. Therefore, the event-triggered mechanisms based on the TBG function can further reduce the consumption of communication resources when $t > t_p$.

3.3 Consensus Analysis

Under the continuous event-triggered communication framework, the control input for DG i is designed as:

$$\begin{aligned} u_i^{\omega}(t) &= (1+k(t))\,[\sum_{j\in N_i} a_{ij}\left(\omega_i(t_k^i)-\omega_j(t_k^j)\right) \\ &\quad + b_i\left(\omega_i(t_k^i)-\omega^*\right)], \\ u_i^{v}(t) &= (1+k(t))\,[\sum_{j\in N_i} a_{ij}\left(v_i(t_k^i)-v_j(t_k^j)\right) \\ &\quad + b_i\left(v_i(t_k^i)-v^*\right)]. \end{aligned} \tag{22}$$

To carry out the following analysis, some useful intermediate variables are employed. For $i \in \mathcal{V}$, define $\hat{\omega}_i(t) = \omega_i(t) - \omega^*$, $\hat{v}_i(t) = v_i(t) - v^*$, $x_i(t) = [\hat{\omega}_i(t), \hat{v}_i(t)]^T$, $X = [x_1, ..., x_n]^T$, $E = [e_1, ..., e_n]^T$. Thus we also have

$$\begin{aligned} u_i(t) = (1+k(t))\,[&\sum_{j\in N_i} a_{ij}\left(e_i(t)-e_j(t)+x_i(t)-x_j(t)\right) \\ &+ b_i\left(e_i(t)+x_i(t)\right)]. \end{aligned} \tag{23}$$

By substituting the control protocols (23), the system (2) can be rewritten as the following compact form

$$\dot{X}(t) = -(1+k(t))\left[\hat{L}\otimes \mathbf{1}_N\right](E+X), \tag{24}$$

where $\otimes$ represents the Kronecker product, $\mathbf{1}_N$ is denotes the n-dimensional column vector with all elements being 1.

Theorem 1. By employing the control (23), for the microgrid systems (24), the practical prescribed-time consensus is achieved.

Proof: Select Lyapunov function

$$V(t) = V_1(t) + V_2(t), \tag{25}$$

where $V_1(t) = \frac{1}{2}X^T(t)X(t), V_2(t) = h\sum_{i=1}^{N}\eta_i(t)$, $h > \frac{\lambda_{\min}(\hat{L})}{4}$.

The derivative of the V_1 is calculated as follows

$$\begin{aligned} \dot{V}_1(t) =& X^T\dot{X} \\ =& X^T\left(-(1+k(t))\left[\hat{L}\otimes\mathbf{1}_N\right](E+X)\right) \\ \leqslant& -(1+k(t))X^T\lambda_{\min}(\hat{L})(E+X) \\ =& -(1+k(t))\lambda_{\min}(\hat{L})(X^TE+X^TX). \end{aligned} \tag{26}$$

Based on Young's inequality, we infer

$$-X^TE \leqslant \frac{c}{2}X^TX + \frac{1}{2c}E^TE, \tag{27}$$

where c is any positive constant, in this paper $c = \frac{\lambda_{\min}(\hat{L})}{2h}$.

Further we have

$$\begin{aligned} \dot{V}_1(t) \leqslant& -(1+k(t))\lambda_{\min}(\hat{L})(1-\frac{c}{2})X^TX \\ &+ (1+k(t))\frac{\lambda_{\min}(\hat{L})}{2c}\sum_{i=1}^{N}(e_i)^2. \end{aligned} \tag{28}$$

It follows from Equation (18) that

$$\begin{aligned} \dot{V}_2(t) =& h\sum_{i=1}^{N}\dot{\eta}_i(t) \\ =& h(1+k(t)(-\sum_{i=1}^{N}\phi_i\eta_i(t) - \sum_{i=1}^{N}\vartheta_i(t)). \end{aligned} \tag{29}$$

Then, we have

$$\begin{aligned}\dot{V}(t) =&\dot{V}_1(t) + \dot{V}_2(t)\\ =&-(1+k(t))\lambda_{\min}(\hat{L})(1-\frac{c}{2})X^TX\\ &-h(1+k(t))\sum_{i=1}^{N}\phi_i\eta_i(t)\\ &-(1+k(t))(h-\frac{\lambda_{\min}(\hat{L})}{2c})\sum_{i=1}^{N}\vartheta_i(t)\\ \leqslant&-(1+k(t))\lambda_{\min}(\hat{L})(1-\frac{1}{2c})X^TX\\ &-h\phi(1+k(t))\sum_{i=1}^{N}\eta_i(t)\\ \leqslant&-(1+k(t))\varepsilon(X^TX+h\sum_{i=1}^{N}\eta_i(t))\\ =&-(1+k(t))\varepsilon V(t),\end{aligned} \tag{30}$$

where $\phi = \min\{\phi_1,...,\phi_n\}$, $\varepsilon = \min\left\{\lambda_{\min}(\hat{L})(1-\frac{1}{2c}),\phi\right\}$. According to Lemma 2, we have

$$V(t) \leqslant e^{-\varepsilon t}\left(\frac{1-\xi(t)+\sigma}{1+\sigma}\right)^{-\varepsilon}V(0). \tag{31}$$

When $t = t_p$, there is

$$V(t_p) \leqslant e^{-\varepsilon t_p}\left(\frac{\sigma}{1+\sigma}\right)^{-\varepsilon}V(0). \tag{32}$$

Obviously, $V(t)$ converges to the boundary at the prescribed time t_p. When $t > t_p$, we have

$$V(t) \leqslant e^{-\varepsilon(t-t_p)}V(t_p). \tag{33}$$

It can be seen from the above equation that when $t > t_p$, $V(t)$ converges to the origin with an exponential convergence rate, and the convergence rate will not be lower than ε.

For $t \in [0, t_p]$, using Lemma 1 and the comparison principle, we can conclude that

$$\begin{aligned}V(t) &\leqslant \left(\frac{\sigma}{1+\sigma}\right)^{-\varepsilon}V(0),\\ V_1(t) &\leqslant \left(\frac{\sigma}{1+\sigma}\right)^{-\varepsilon}V(0).\end{aligned} \tag{34}$$

Furthermore, we obtain that

$$\lim_{t\to t_p}\|X\| \leqslant \sqrt{2\left(\frac{\sigma}{(1+\sigma)}\right)^{-\varepsilon}V(0)}. \tag{35}$$

Therefore,

$$\begin{cases}\lim_{t\to t_p}|\omega_i(t)-\omega^*| = \delta_1,\\ \lim_{t\to t_p}|v_i(t)-v^*| = \delta_2.\end{cases} \tag{36}$$

This demonstrates the frequency and voltage at which t_p enters the boundary. This implies that the state disagreement can be systematically regulated to a desired level through proper selection of the control parameter σ in (23). For all $t > t_p$, when $\xi(t) = 0$, the Lyapunov function derivative satisfies $V_1(t) \leq -\varepsilon V(t)$, which implies that $V_1(t)$ is non-increasing. Therefore, $V_1(t)$ converges exponentially within the boundary. Further we have

$$\begin{cases}\lim_{t\to+\infty}|\omega_i(t)-\omega^*| = 0,\\ \lim_{t\to+\infty}|v_i(t)-v^*| = 0.\end{cases} \tag{37}$$

The microgrid system realize the practical prescribed-time consensus for frequency and voltage. Proof completes.

Remark 5. According to Equation (35), the convergence error $\sqrt{2\left(\frac{\sigma}{1+\sigma}\right)^{-\varepsilon}V(0)}$ can be adjusted by regulating the parameter σ. In addition, the consensus time t_p can be realised by designing different time base generator function $\xi(t)$. Moreover, by introducing the dynamic event triggered strategy, the system communication resources can be greatly saved. In general, the controller we designed can achieve both practical prescribed-time consensus and save communication resources, which can improve the control performance of the whole microgrid.

Remark 6. It is worth noting that both the consensus time and the convergence accuracy can be adjusted arbitrarily by the designer. This kind of arbitrary adjustability is very significant in frequency regulation and voltage regulation problems of real power systems. Since the power system is limited by physical equipment and environment, approximate solutions are more practical than exact solutions.

It will be shown below that every agent does not have the Zeno behavior. This implies that the event-triggering condition (16) guarantees a strictly positive minimum trigger interval for all agents in the system. The following theorem formally establishes this result.

Theorem 2. Under the trigger conditions(16), for the system(25), Zeno behaviour is nonexistent.

Proof: When $t \in \left[t_k^i, t_{k+1}^i\right)$, The upper right Dini derivative of $e_i(t)$ is

$$D^+ e_i(t) = -\dot{x}_i(t). \tag{38}$$

From the trigger conditions, we have $e_i\left(t_k^i\right) = 0$, thus

$$\begin{aligned} e_i^2(t) =& (\int_{t_k^i}^{t} |\dot{x}_i(t)|ds)^2 \\ \leqslant& (\int_{t_k^i}^{t} || \left(1 + k(t)\right) \left[\hat{L} \otimes \mathbf{1}_N\right] || \\ & |(e_i(s) + x_i(s))|ds)^2. \end{aligned} \tag{39}$$

Since the $k(t)$ we construct is bounded for $t \in [0, t_p)$, we define that there is a $m > 0$, which satisfies $|| \left(1 + k(t)\right) \left[\hat{L} \otimes \mathbf{1}_N\right] || \leqslant m$. Therefore,

$$e_i^2(t) \leqslant (\int_{t_k^i}^{t} m(|(e_i(s)| + |x_i(s))|)ds)^2. \tag{40}$$

Take the limit on both sides, we have

$$\lim_{t \to t_{k+1}^i} |e_i(t)|^2 \leqslant \lim_{t \to t_{k+1}^i} (\int_{t_k^i}^{t} m(|e_i(s)| + |x_i(s)|)ds)^2. \tag{41}$$

From Theorem 1, we have

$$\begin{aligned} V_1 = \frac{1}{2} X^T X < e^{-\varepsilon t} \left(\frac{1 - \varepsilon(t) + \sigma}{1 + \sigma}\right)^{-\varepsilon} V(0) \\ \sum_{i=1}^{N} x_i(t) \leqslant e^{-\varepsilon t} \left(\frac{1 - \varepsilon(t) + \sigma}{1 + \sigma}\right)^{-\varepsilon} V(0). \end{aligned} \tag{42}$$

It can be seen that there is a maximum upper bound for $\sum_{i=1}^{N} x_i(t)$. Further we can conclude that x_i must also have an upper bound. We define $||x_i(t)|| \leqslant M$. In addition, according to the designed event trigger threshold function we have $|e_i(t)| < \sqrt{\frac{\eta_i(t)}{\kappa_i}}$ when $t \in \left[t_k^i, t_{k+1}^i\right)$, and the $\eta_i(t)$ function is strictly monotonically decreasing.

Further we have

$$\begin{aligned} \eta_i(t_{k+1}^i) \leqslant (t_{k+1}^i - t_k^i)^2 m^2 (\sqrt{\frac{\eta_i(t_{k+1}^i)}{\kappa_i}} + M)^2, \\ \frac{\eta_i(t_{k+1}^i)}{m^2 (\sqrt{\frac{\eta_i(t_{k+1}^i)}{\kappa_i}} + M)^2} \leqslant (t_{k+1}^i - t_k^i)^2. \end{aligned} \tag{43}$$

Combine the threshold function we know

$$\eta_i(t) > \eta_i(0) e^{-(\phi_i + 1/\kappa_i)} \left(1 - \frac{\xi(t)}{1 + \sigma}\right)^{\phi_i + 1/\kappa_i} > 0. \tag{44}$$

Thus

$$t_{k+1}^i - t_k^i > 0. \tag{45}$$

Therefore, there always is a number ϵ small enough to $\epsilon \leqslant t_{k+1}^i - t_k^i$, which means that there is a minimum trigger interval. Hence there is no Zeno behaviour. Proof completes.

Remark 7. In [31], it demonstrates that Zeno behavior is excluded throughout the entire time domain except for the specific moment $t = t_p$. At this particular instant, since it is impossible to determine whether $k(t)$ remains bounded, the analytical approach employed cannot effectively determine the existence of Zeno behavior . In contrast, the controller proposed in this paper completely avoids singularity issues at any time instant. This is achieved by introducing a sufficiently small constant σ in the denominator of the function $k(t)$, which ensures that $k(t)$ remains bounded at $t = t_p$, thereby guaranteeing the boundedness of $|| \left(1 + k(t)\right) \left[\hat{L} \otimes \mathbf{1}_N\right] ||$. Consequently, we can more easily conclude that the system is not subject to Zeno behavior at any moment.

4 Numerical simulations

This section presents numerical simulations based on the microgrid test system described in [12]. The configuration and communication architecture of the microgrid test system are illustrated in Figures 2 and 3. The microgrid test system comprises four DGs and four transmission lines. According to the communication topology in Figure 3, the corresponding Laplacian matrix L and concatenation matrix B are represented as follows:

$$L = \begin{bmatrix} 1 & -1 & 0 & 0 \\ -1 & 2 & -1 & 0 \\ 0 & -1 & 2 & -1 \\ 0 & 0 & -1 & 1 \end{bmatrix}, \tag{46}$$

$$B = \begin{bmatrix} 1 & 0 & 0 & 0 \\ 0 & 0 & 0 & 0 \\ 0 & 0 & 0 & 0 \\ 0 & 0 & 0 & 0 \end{bmatrix}. \tag{47}$$

Set only DG1 to directly receive reference signals from the upper control, where frequency reference signal $\omega = 314.16$rad/s, voltage reference signal $v = 380$V. Besides, the initial states of microgrid system are $\omega_1(0) = 316$rad/s, $\omega_2(0) = 312$rad/s, $\omega_3(0) = 313$rad/s, $\omega_4(0) = 315$rad/s and $v_1(0) = 385$V, $v_2(0) = 382$V, $v_3(0) = 375$V, $v_4(0) = 377$V.

The parameters of the trigger condition in (16) are chosen as $\eta(0) = [2, 3, 2, 3]^T, \phi_1 = \phi_2 = 1.1, \phi_3 = \phi_4 = 0.9, \kappa_1 = \kappa_2 = \kappa_3 = \kappa_4 = 1$. In addition, the following time base generator function is considered as

$$\xi(t) = \begin{cases} -\frac{1}{500}t^3 + \frac{3}{100}t^2, & 0 \le t \le t_p \\ 1, & t > t_p \end{cases} \tag{48}$$

where the prescribed time $t_p = 10$s. It is obtained from Theorem 1 that the microgrid test system achieves the practical prescribed time consensus and the estimation of the settling time is $t = 10$s.

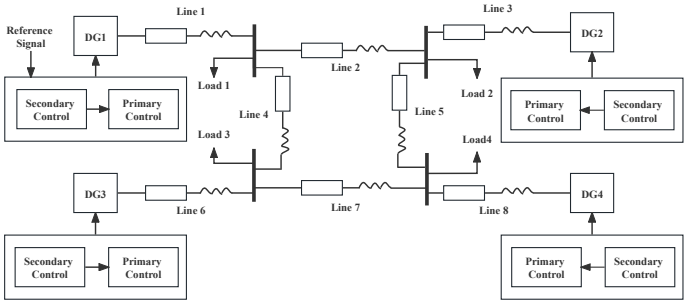

Figure 2. Microgrid test system structure.

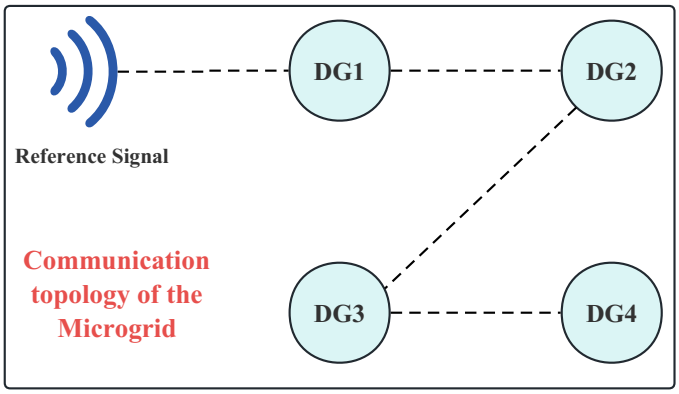

Figure 3. Communication topology of the microgrid.

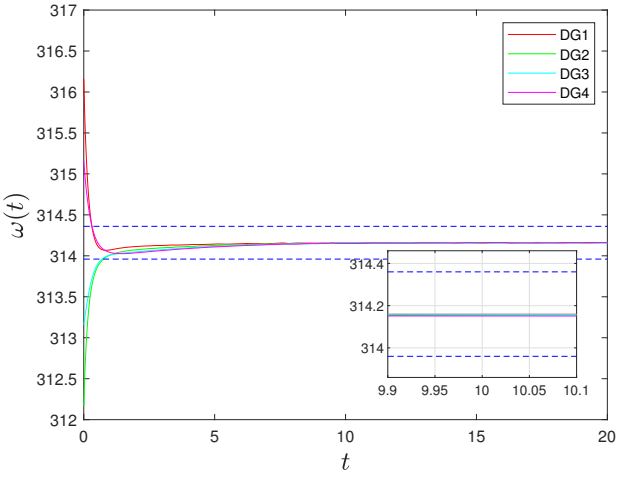

(a)Frequency control

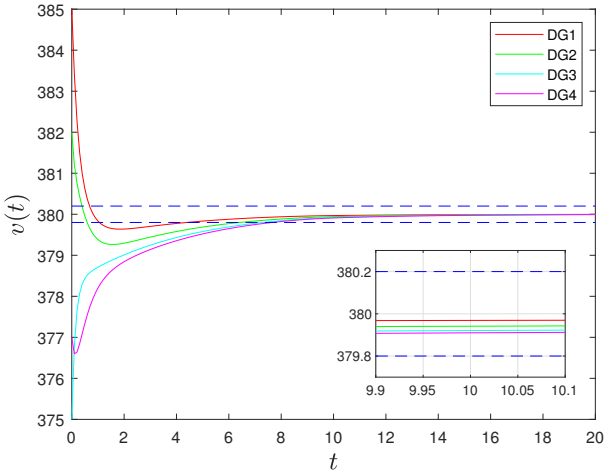

(b)Voltage control

Figure 4. States trajectories of each DG under the controller (14).

As shown in the Figure 4, the frequency and voltage output values are regulated to the corresponding rated operating values $\omega_{ref} = 314.16$rad/s and $v_{ref} = 380$V under the action of the controller (14). In addition, when $t = 10$s the frequency and voltage converge to the boundary. Thus the Microgrid system realizes the practical prescribed time consensus at the prescribed time $t_p = 10$s.

Figure 5 shows the frequency and voltage of the microgrid output under the effect of the controller (23) during event-triggered communication. It can be noticed that the output effect of Figure 5 is almost the same as that of Figure 4. However, it consumes less communication resources than Figure 4 due to introduce the event-triggered mechanism.

Accordingly, the distribution of event-triggered time for each DG under the event-triggered mechanism is shown in Figure 6. It can be seen that the controller update of each DG is asynchronous, with controller updates only performed when it needs to renew its own state. This greatly reduces the frequency of controller updates and thus saves communication resources. In order to visualize the advantages of our designed event-triggered strategy, the time interval of each trigger of DG1 is shown in Figure 7. Obviously, the trigger interval of DG1 becomes larger when $t >$ 10s, which means less communication is required. It is further verified that the event-triggered strategy based on TBG designed in this paper can reduce the consumption of communication resources after $t =$ 10s.

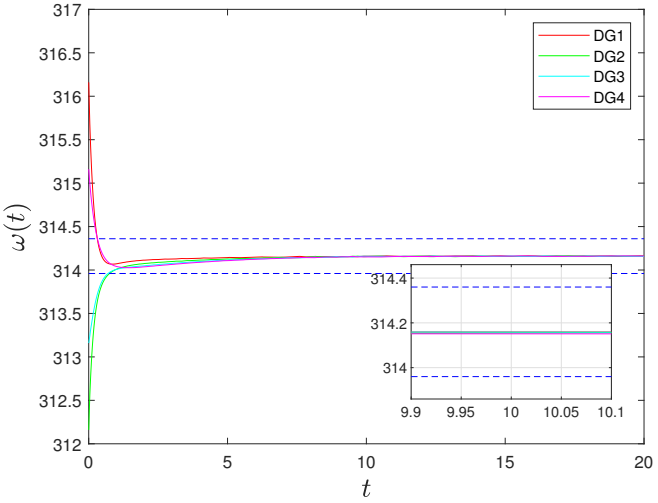

(a)Frequency control

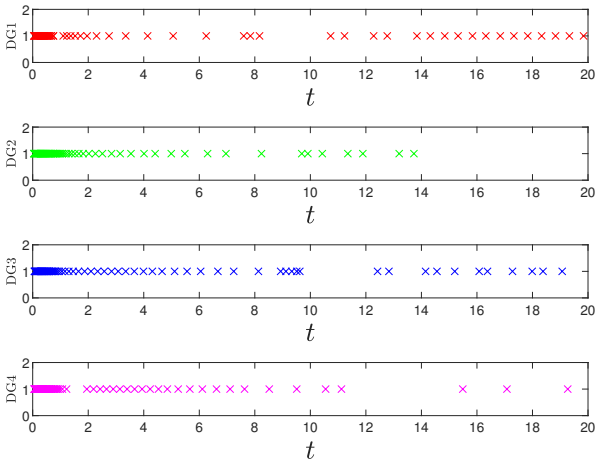

(a)Trigger time of frequency control

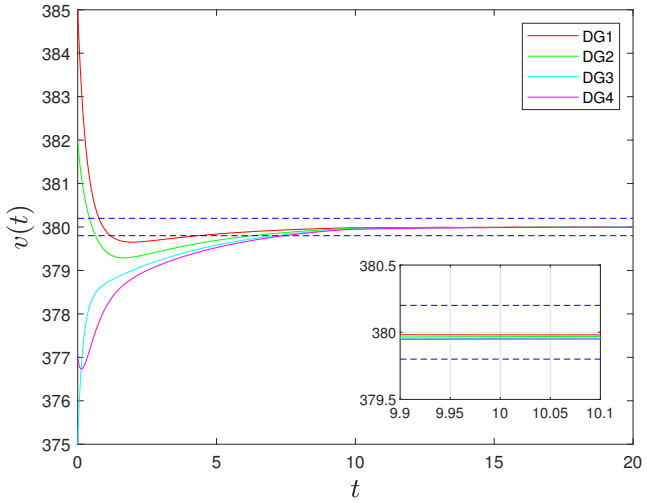

(b)Voltage control

Figure 5. States trajectories of each DG under the controller (23).

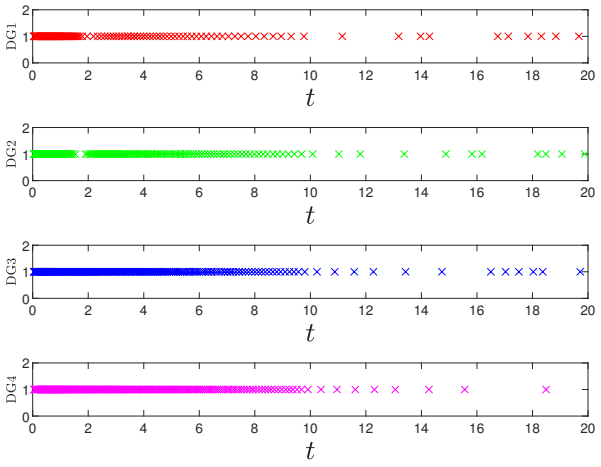

(b)Trigger time of voltage control

Figure 6. Trigger time of each DG.

To better validate the superiority of the proposed controller and event-triggered mechanism, we compared the proposed algorithm (Algorithm 1) in this paper with an existing distributed event-triggered fixed-time consensus algorithm (Algorithm 2). Simulation experiments were conducted using the same system parameters as those in Algorithm 1. Figures 8-10 demonstrate the frequency and voltage of the microgrid output, the triggering instants of each DG, and the triggering intervals of DG1 under Algorithm 2, respectively. Both Algorithm 1 and Algorithm 2 can ensure system convergence to the prescribed bound. However, based on the calculated settling time where $t = 17s > t_p = 10s$, it can be observed that the settling time computed by Algorithm 1 is closer to the actual convergence time, indicating that Algorithm 1 exhibits less conservatism in settling time estimation. To evaluate the communication resource occupancy, a comparison between Figure 6 and Figure 9 reveals that the triggering sequence in Figure 6 is sparser, demonstrating that the design of dynamic event-triggering through the introduction of a TBG function effectively reduces the triggering rate. In Figure 10, the overall triggering intervals of Algorithm 2 are relatively small, none exceeding $0.5s$. By comparing Figure 7 and Figure 10, it can be seen that under Algorithm 1, the controller's triggering intervals are longer. This further verifies that the proposed dynamic event-triggering strategy based on the TBG function can effectively reduce communication resource consumption while maintaining control

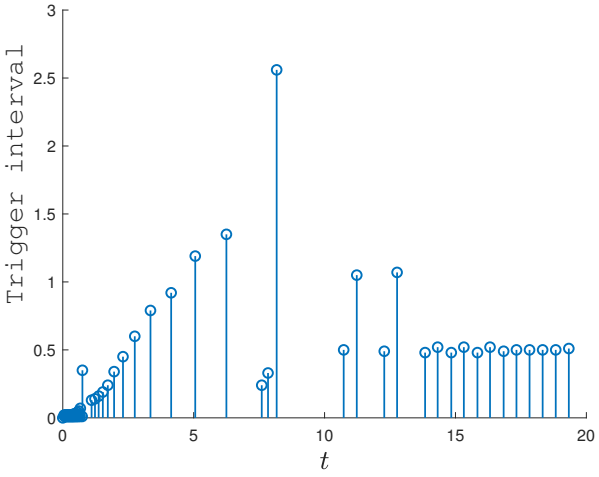

(a)Trigger interval of frequency control

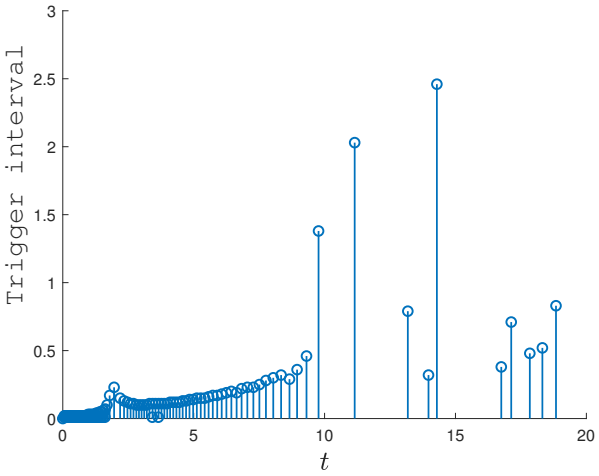

(b)Trigger interval of voltage control

Figure 7. Trigger interval of DG1.

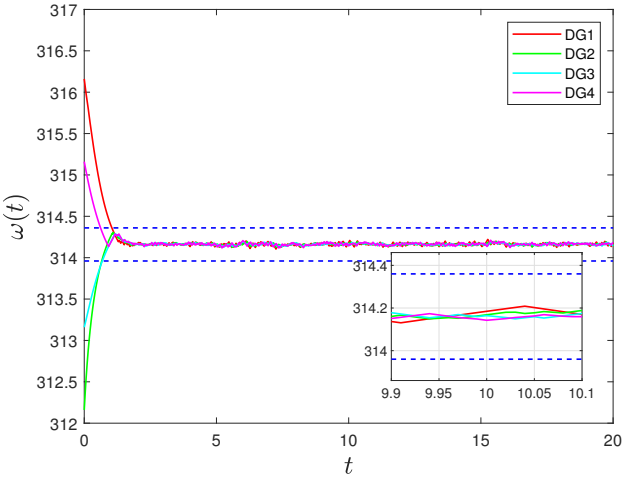

(a)Frequency control

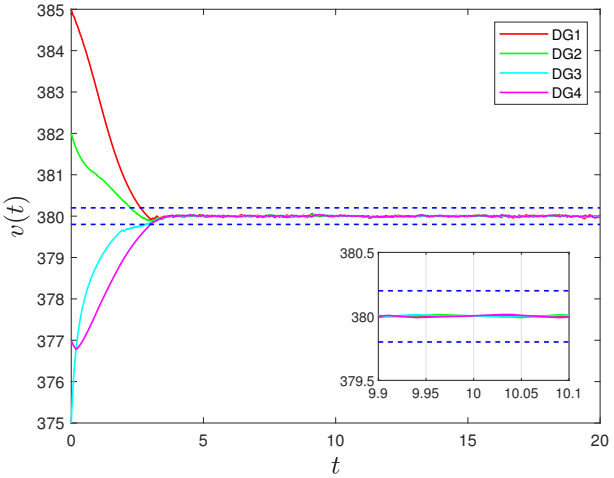

(b)Voltage control

Figure 8. States trajectories of each DG under the distributed event-triggered fixed-time consensus algorithm.

performance.

Based on the Simulink simulation platform, the robustness of the proposed algorithm against external disturbances such as load variations was validated. Two loads were integrated into the microgrid system illustrated in Figure 2, with parameter settings adopted from [35]. The simulation procedure was configured as follows: Phase 1 ($0s$–$5s$): Only the primary control was active. The introduction of the loads caused a decrease in both frequency and voltage. Phase 2 ($5s$–$10s$): The loads remained connected, and both the primary control and the distributed secondary control were activated. Phase 3 (after $10s$): One load was disconnected, leaving only one load in operation, while both primary and secondary controls remained active. The simulation results, presented in Figure 11, show the response curves of voltage and frequency under varying load conditions. As observed in the Figure 11, both voltage and frequency initially remained at their reference values. At $t = 5s$, the connection of the loads led to a decline in voltage and frequency due to the droop characteristics. To restore them to the reference values, the distributed secondary control algorithm was activated after $5s$. The results demonstrate that both voltage and frequency gradually returned to their reference values, confirming the effectiveness of the proposed distributed algorithm. After $10s$, when one load was disconnected, brief fluctuations occurred in the voltage and frequency of each distributed generator. Subsequently, however, the system states quickly readjusted and tracked the reference signals again. This indicates that even under load variation scenarios, the proposed algorithm is capable of achieving consensus among system states

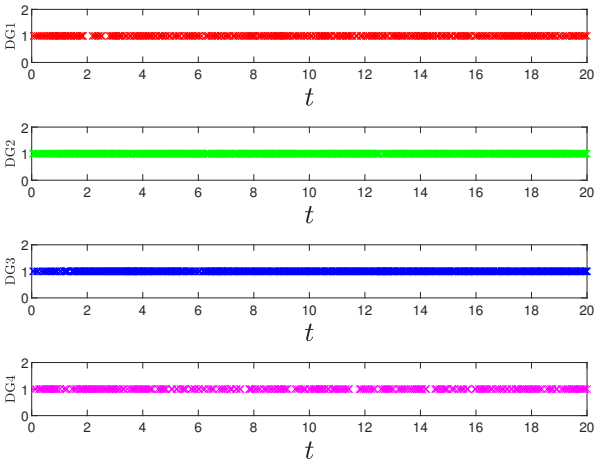

(a)Trigger time of frequency control

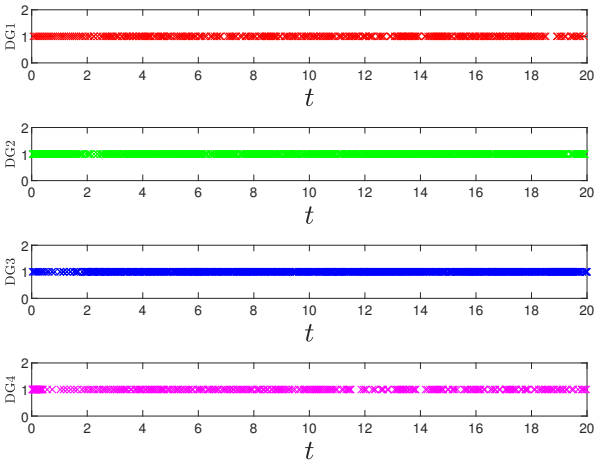

(b)Trigger time of voltage control

Figure 9. Trigger time of each DG under the distributed event-triggered fixed-time consensus algorithm.

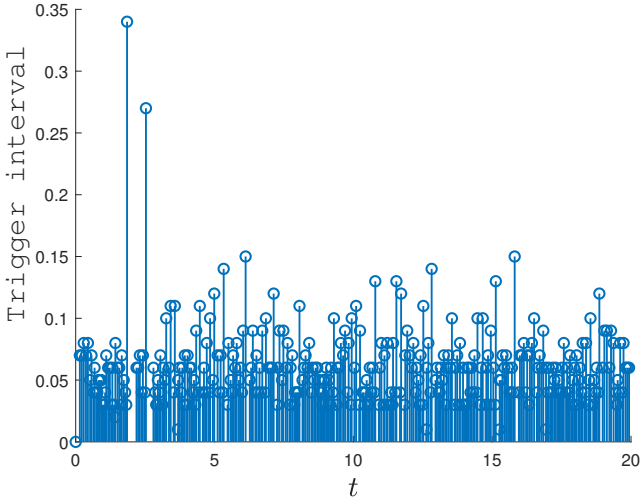

(a)Trigger interval of frequency control

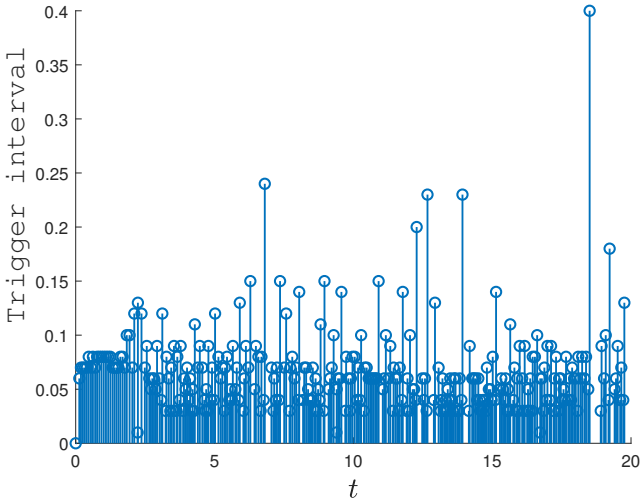

(b)Trigger interval of voltage control

Figure 10. Trigger interval of DG1 under the distributed event-triggered fixed-time consensus algorithm.

within the prescribed time $t_p = 15s$.

Remark 8. It is worth pointing out that predefined time stability means that the system can reach stability at or before a prescribed time, not just at the prescribed time, as shown in Figure 4. This means that the prescribed time controller enables explicit specification of an upper bound on the consensus convergence time. This guarantees that all system states will achieve agreement at or before the prescribed time. While theoretical analysis demonstrates asymptotic convergence to the equilibrium point at the prescribed time, practical implementation reveals that the actual convergence characteristics are influenced by several implementation factors. Therefore, under the premise of satisfying the sufficient conditions for designing the prescribed time controller, the controlled state can be made to converge quickly before the prescribed time by reasonably adjusting the control parameters. It should be noted that although the finite/fixed time stability can complete the convergence of the controlled state within a certain time. However, the convergence time cannot be predetermined a priori, as it is dependent on the initial value of system state, the system parameters and other implementation-dependent factors.

Remark 9. Simulation experiments were conducted using different forms of TBG functions, specifically trigonometric and exponential functions. The results demonstrate that the choice of function form has negligible influence on both the convergence speed and control accuracy of the system. It should be

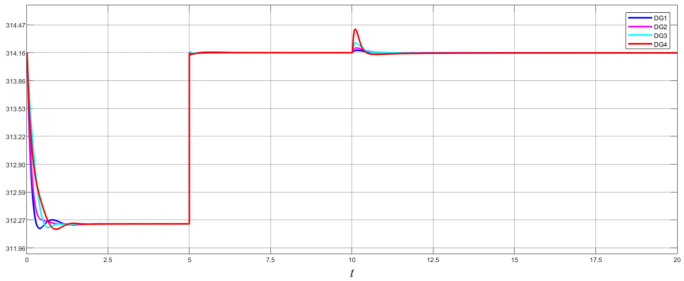

(a)Frequency response curve when load changes

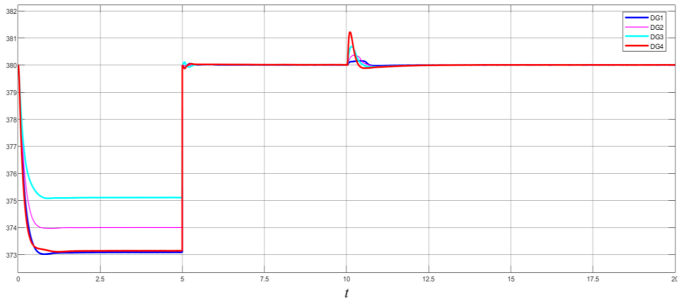

(b)Voltage response curve when load changes

Figure 11. States trajectories of each DG under the controller (23) when load changes.

noted, however, that this conclusion is drawn from simulation studies. The impact of different TBG function forms on the secondary control of microgrids in real industrial environments remains a subject for further investigation.

Remark 10. The prescribed-time control developed in this paper requires the system states to converge within a predefined bound before the prescribed-time T_p, which typically demands continuous high-frequency control updates. In contrast, the event-triggered strategy reduces resource consumption via aperiodic communication. These two approaches are synergized through the TBG function. It is rigorously proven via Lyapunov stability theory that even with event-triggered communication the system states converge within the predesigned bounds prior to T_p. Moreover, the boundedness of $k(t)$ is employed to demonstrate the existence of a minimum inter event time, thereby avoiding Zeno behavior. Compared to fixed periodic communication, the event-triggered strategy significantly reduces the number of communication instances when the system states are far from equilibrium, effectively achieving the primary goal of communication resource conservation. The convergence time remains exactly the prescribed-time T_p, unaffected by the communication strategy. The system enables intelligent allocation of communication resources: lower frequency communication during the initial phase requiring large adjustments, and higher frequency communication for a very short duration during the final phase requiring precise fine tuning. Overall, this approach still achieves significant resource savings.

5 Conclusion

In this paper, based on the improved event-triggered mechanism, a new distributed control algorithm has been designed to realize the practical prescribed-time consensus of the microgrid system. Moreover, it has been proved that the microgrid still achieves the practical prescribed time consensus under the event-triggered communication mechanism. Furthermore, Zeno behavior does not occur. Finally, the effectiveness of the proposed control algorithm has been verified by simulation examples. Future research will focus on designing more appropriate distributed control algorithms and event-triggered communication mechanisms to solve the microgrid distributed power optimization problem.

Data Availability Statement

Data will be made available on request.

Funding

This work was supported in part by the National Natural Science Foundation of China under Grant 62473348; in part by the Guangdong Basic and Applied Basic Research Foundation under Grant 2025A1515011111; in part by the Fundamental Research Funds for National Universities, China University of Geosciences (Wuhan) under Grant 2024XLB37.

Conflicts of Interest

The authors declare no conflicts of interest.

Ethical Approval and Consent to Participate

Not applicable.

References

[1] Uddin, M., Mo, H., Dong, D., Elsawah, S., Zhu, J., & Guerrero, J. M. (2023). Microgrids: A review, outstanding issues and future trends. *Energy Strategy Reviews, 49*, 101127. [Crossref]

[2] Hu, J., Shan, Y., Cheng, K. W., & Islam, S. (2022). Overview of power converter control in microgrids—Challenges, advances, and future trends. *IEEE Transactions on Power Electronics, 37*(8), 9907-9922. [Crossref]

[3] Espina, E., Llanos, J., Burgos-Mellado, C., Cardenas-Dobson, R., Martinez-Gomez, M., & Saez, D. (2020). Distributed control strategies for microgrids: An overview. *IEEE Access, 8*, 193412-193448. [Crossref]

[4] Ning, B., Han, Q. L., Zuo, Z., Ding, L., Lu, Q., & Ge, X. (2022). Fixed-time and prescribed-time consensus control of multiagent systems and its applications: A survey of recent trends and methodologies. *IEEE Transactions on Industrial Informatics, 19*(2), 1121-1135. [Crossref]

[5] Ge, X., & Han, Q. L. (2017). Distributed formation control of networked multi-agent systems using a dynamic event-triggered communication mechanism. *IEEE Transactions on Industrial Electronics, 64*(10), 8118-8127. [Crossref]

[6] Wang, X., Wang, G., & Li, S. (2020). A distributed fixed-time optimization algorithm for multi-agent systems. *Automatica, 122*, 109289. [Crossref]

[7] Zaery, M., Wang, P., Wang, W., & Xu, D. (2021). A novel fully distributed fixed-time optimal dispatch of DC multi-microgrids. *International Journal of Electrical Power & Energy Systems, 129*, 106792. [Crossref]

[8] Zhang, R., & Hredzak, B. (2018). Distributed finite-time multiagent control for DC microgrids with time delays. *IEEE Transactions on Smart Grid, 10*(3), 2692-2701. [Crossref]

[9] Dehkordi, N. M., Sadati, N., & Hamzeh, M. (2016). Distributed robust finite-time secondary voltage and frequency control of islanded microgrids. *IEEE Transactions on Power systems, 32*(5), 3648-3659. [Crossref]

[10] Ning, B., Han, Q. L., & Ding, L. (2020). Distributed finite-time secondary frequency and voltage control for islanded microgrids with communication delays and switching topologies. *IEEE Transactions on Cybernetics, 51*(8), 3988-3999. [Crossref]

[11] Polyakov, A. (2011). Nonlinear feedback design for fixed-time stabilization of linear control systems. *IEEE transactions on Automatic Control, 57*(8), 2106-2110. [Crossref]

[12] Liu, L. N., & Yang, G. H. (2022). Distributed fixed-time optimal resource management for microgrids. *IEEE Transactions on Automation Science and Engineering, 20*(1), 404-412. [Crossref]

[13] Zeng, Y., Zhang, Q., Liu, Y., Guo, H., Liu, S., Zhang, F., ... & Yu, H. (2023). Fixed-time secondary controller for rapid state-of-charge balancing and flexible bus voltage regulation in DC microgrids. *IEEE Transactions on Power Systems, 39*(3), 5393-5407. [Crossref]

[14] Ma, L., Hu, C., Yu, J., Wang, L., & Jiang, H. (2022). Distributed fixed/preassigned-time optimization based on piecewise power-law design. *IEEE Transactions on Cybernetics, 53*(7), 4320-4333. [Crossref]

[15] Sahoo, S., Mishra, S., Fazeli, S. M., Li, F., & Dragičević, T. (2019). A distributed fixed-time secondary controller for DC microgrid clusters. *IEEE Transactions on Energy Conversion, 34*(4), 1997-2007. [Crossref]

[16] Wang, P., Huang, R., Zaery, M., Wang, W., & Xu, D. (2020). A fully distributed fixed-time secondary controller for DC microgrids. *IEEE Transactions on Industry Applications, 56*(6), 6586-6597. [Crossref]

[17] Yuan, Q. F., Wang, Y. W., Liu, X. K., & Lei, Y. (2021). Distributed fixed-time secondary control for DC microgrid via dynamic average consensus. *IEEE Transactions on Sustainable Energy, 12*(4), 2008-2018. [Crossref]

[18] Wang, L., Zeng, Z., & Ge, M. F. (2019). A disturbance rejection framework for finite-time and fixed-time stabilization of delayed memristive neural networks. *IEEE Transactions on Systems, Man, and Cybernetics: Systems, 51*(2), 905-915. [Crossref]

[19] Zhang, H., Chen, Z., Ye, T., Yue, D., Xie, X., Hu, X., ... & Xue, Y. (2023). Security event-trigger-based distributed energy management of cyber-physical isolated power system with considering nonsmooth effects. *IEEE Transactions on Cybernetics, 54*(6), 3553-3564. [Crossref]

[20] Zhang, H., Yue, D., Dou, C., Xue, Y., & Hancke, G. P. (2022). Event-trigger-based distributed optimization approach for two-level optimal model of isolated power system with switching topology. *IEEE Transactions on Systems, Man, and Cybernetics: Systems, 53*(4), 2339-2349. [Crossref]

[21] Wu, Y. D., Ge, M. F., Liu, Z. W., Zhang, W. Y., & Wei, W. (2021). Distributed CPS-based secondary control of microgrids with optimal power allocation and limited communication. *IEEE Transactions on Smart Grid, 13*(1), 82-95. [Crossref]

[22] Qian, T., Liu, Y., Zhang, W., Tang, W., & Shahidehpour, M. (2019). Event-triggered updating method in centralized and distributed secondary controls for islanded microgrid restoration. *IEEE Transactions on Smart Grid, 11*(2), 1387-1395. [Crossref]

[23] Li, Z., Cheng, Z., Liang, J., Si, J., Dong, L., & Li, S. (2019). Distributed event-triggered secondary control for economic dispatch and frequency restoration control of droop-controlled AC microgrids. *IEEE Transactions on Sustainable Energy, 11*(3), 1938-1950. [Crossref]

[24] Chen, M., Xiao, X., & Guerrero, J. M. (2017). Secondary restoration control of islanded microgrids with a decentralized event-triggered strategy. *IEEE Transactions on Industrial Informatics, 14*(9), 3870-3880. [Crossref]

[25] Zhang, J., Yang, J., Zhang, Z., & Wu, Y. (2023).

Practical prescribed time control for state constrained systems with event-triggered strategy: settling time regulator-based approach. *International Journal of Robust and Nonlinear Control, 33*(3), 1838-1857. [Crossref]

[26] Zhou, S., Song, Y., & Wen, C. (2021). Event-triggered practical prescribed time output feedback neuroadaptive tracking control under saturated actuation. *IEEE Transactions on Neural Networks and Learning Systems, 34*(8), 4717-4727. [Crossref]

[27] Ning, P., Hua, C., Li, K., & Meng, R. (2023). Event-triggered control for nonlinear uncertain systems via a prescribed-time approach. *IEEE Transactions on Automatic Control, 68*(11), 6975-6981. [Crossref]

[28] Yu, H., & Hao, F. (2020). The existence of Zeno behavior and its application to finite-time event-triggered control. *Science China. Information Sciences, 63*(1), 139201. [Crossref]

[29] Ning, B., Han, Q. L., & Zuo, Z. (2019). Practical fixed-time consensus for integrator-type multi-agent systems: A time base generator approach. *Automatica, 105*, 406-414. [Crossref]

[30] Zhang, X., Liu, L., & Feng, G. (2015). Leader–follower consensus of time-varying nonlinear multi-agent systems. *Automatica, 52*, 8-14. [Crossref]

[31] Chen, X., Yu, H., & Hao, F. (2020). Prescribed-time event-triggered bipartite consensus of multiagent systems. *IEEE Transactions on Cybernetics, 52*(4), 2589-2598. [Crossref]

[32] Hardy, G. H., Littlewood, J. E., & Pólya, G. (1952). *Inequalities*. Cambridge university press.

[33] Wang, Y., Song, Y., Hill, D. J., & Krstic, M. (2018). Prescribed-time consensus and containment control of networked multiagent systems. *IEEE transactions on cybernetics, 49*(4), 1138-1147. [Crossref]

[34] Xu, C., Xu, H., Guan, Z. H., & Ge, Y. (2022). Observer-based dynamic event-triggered semiglobal bipartite consensus of linear multi-agent systems with input saturation. *IEEE Transactions on Cybernetics, 53*(5), 3139-3152. [Crossref]

[35] Bidram, A., Davoudi, A., Lewis, F. L., & Qu, Z. (2013). Secondary control of microgrids based on distributed cooperative control of multi-agent systems. *IET Generation, Transmission & Distribution, 7*(8), 822-831. [Crossref]

Houlang He received the B.S. degree in automation from South-Central Minzu University, Wuhan, China, in 2024. He is currently working toward the M.S. degree in School of Automation, China University of Geosciences, Wuhan, China. (Email: 2813426514@qq.com)

Yu Zhou received the B.S. degree in materials forming and control engineering from Anhui University of Technology, Anhui, China, in 2022, and the M. S. degree in electronic information from School of Automation, China University of Geosciences, Wuhan, China, in 2025. (Email: 1169573955@qq.com)

Guanghui Jiang received the B.S. degree in automation from China University of Geosciences, Wuhan, China, in 2023. He is currently working toward the Ph.D. degree in School of Automation, China University of Geosciences, Wuhan, China. His current research interests include dynamics of neural networks, stochastic systems, and finite-time control. (Email:jiangguanghui@cug.edu.cn)

Leimin Wang received the B.S. degree in mathematics and applied mathematics from South-Central Minzu University, Wuhan, China, in 2011, and the Ph.D. degree in control science and engineering from Huazhong University of Science and Technology, Wuhan, in 2016. From December 2018 to December 2019, he was a Visiting Research Fellow with the Department of Electrical, Computer and Biomedical Engineering, University of Rhode Island, Kingston, RI, USA. He is currently a Professor with the School of Automation, China University of Geosciences, Wuhan. His current research interests include dynamics of neural networks, memristive systems, and finite-time control. (Email:wangleimin@cug.edu.cn)